Conformational analysis by NMR spectroscopy and molecular simulation in water of methylated glutamic acids, agonists at glutamate receptors

Nathalie Todeschi,[a] Josyane Gharbi-Benarous,[a,b] Francine Acher,[a] Robert Azerad[a] and Jean-Pierre Girault*,[a]

[a] *Université René Descartes-Paris V, Laboratoire de Chimie et Biochimie Pharmacologiques et Toxicologiques (URA 400 CNRS), 45 rue des Saints-Pères, 75270 Paris Cedex 06, France*
[b] *Université Denis Diderot-Paris VII, UFR Chimie, 2 Place Jussieu, F-75251 Paris Cedex 05, France*

We have undertaken a conformational analysis by ^1H and ^{13}C NMR spectroscopy and molecular modelling of five glutamic acid analogues substituted in position-3 or -4 by a methyl (3T, 3E, 4T, 4E) or a methylene group (4M). These analogues interact with glutamate receptors of the central nervous system, especially the ligand 4T, at one cloned metabotropic receptor ($mGluR_{1a}$), and the ligand 4E, at the ionotropic receptor (KA). A combination of one- and two-dimensional NMR techniques was used to completely assign the ^1H and ^{13}C NMR chemical shifts of the different isomers according to the geometrical isomerism of the methyl. Hetero- and homo-nuclear coupling constants were measured in order to assign the diastereotopic methylene protons at C(3) or C(4), and used for comparison in molecular dynamics (MD) simulations. The system with two carbon–carbon single bonds allows the possibility of *trans* and *gauche* forms 'A, B, C' and 'a, b, c' corresponding to the $\chi 1$ and $\chi 2$ backbone torsion angles, respectively. The hydrogen-bonding possibility, steric effect or electrostatic interaction may be a considerable influence in stabilizing the different conformations in D_2O solution. The conformations may be grouped by the two characteristic distances between the potentially active functional groups, $\alpha N^+ \cdots \gamma CO_2^-$ (d_1) and $\alpha CO_2^- \cdots \gamma CO_2^-$ (d_2) and by the two backbone torsion angles, $\chi 1$ [α-CO_2^-–C(2)–C(3)–C(4)] and $\chi 2$ [$^+$NC(2)–C(3)–C(4)–γCO_2^-].

Introduction

Glutamate receptors play an important role in neuronal plasticity and neurotoxicity in the central nervous system (CNS).[1,2] Glutamic acid is very important in synaptic transmission[3] and plays a major role in essential processes such as learning, memory and some neurobiological disorders such as Huntington and Alzheimer's diseases.[3] Glutamate receptors are classified into two distinct groups, termed ionotropic and metabotropic receptors (mGluRs) on the basis of electrophysiological and pharmacological studies.[2]

The ionotropic receptors, comprising glutamate-gated, cation-specific channel complexes, are subdivided into NMDA receptors which have a particular affinity for *N*-methyl-D-aspartic acid and non-NMDA receptors such as KA (kainic acid) and AMPA (α-amino-3-hydroxy-5-methylisoxazole-4-propionic acid) receptors.[2,4]

The selective agonist *trans*-ACPD[5] has allowed the metabotropic excitatory amino acid receptors to be distinguished pharmacologically from ionotropic receptors and only a few specific drugs were shown to interact with the metabotropic Glu receptors. Recent molecular cloning studies have revealed eight different subtypes of metabotropic receptors[6] (mGluRs) termed mGluR1 to mGluR8. Interestingly, these receptors are involved in glutamate-induced synaptic plasticity and in spatial and olfactory memory. Today, eight mGluRs have been characterized and classifed into three groups based on their sequence homology, transduction mechanism and memory. Group I is composed of mGluR1 and mGluR5, group II[7,8] of mGluR2 and mGluR3 and group III of all other mGluRs. The metabotropic glutamate receptors are coupled to phospholipase C (group I) or negatively coupled to adenylyl cyclase (group II and III).[7,9] Group I is activated by (1*S*,3*R*)-*trans*-ACPD and quisqualate, group II[7,8] by (1*S*,3*R*)-*trans*-ACPD and L-CCGI and group III is selectively activated by L-AP4.[8-13]

In this study, we have undertaken a conformational analysis by ^1H and ^{13}C NMR spectroscopy and molecular modelling of five glutamic acid derivatives (**3T**, **3E**, **4T**, **4E**, **4M**) [Fig. 1(*a*)] substituted in position β- or 3 and γ- or 4 by a methyl (**3T**, **3E**, **4T**, **4E**) or a methylene (**4M**) group and for which the biological activities have been described. These structural changes would not be expected to give rise to important modifications but apparently they profoundly affect the interaction with the receptors. Thus, their individual conformational behaviour in aqueous solution is interesting to investigate.

The five substituted (**3T**, **3E**, **4T**, **4E**, **4M**) derivatives have been tested on the 'mGluR1a' cloned receptor[13] and only one isomer, **4T** [(2*S*,4*S*)-4-methylglutamic acid], revealed similar activity as glutamate, thus suggesting the existence of a particular pharmacological profile. The introduction of a methyl group at the 4-position, resulting in conformational changes of the molecules, enhances selectivity at the ionotropic receptor. Derivative **4E** [(2*S*,4*R*)-4-methylglutamic acid], was identified as having exceptional selectivity for KA receptor subtype with an IC_{50} for inhibition of [^{3}H]-KA binding comparable to kainic acid itself.[14]

Besides their activity at glutamate receptors, these methylated, partially constrained, glutamate analogues are very interesting because of the perceived role of these compounds as good substrates of glutamine synthetase[15] (**3T** and **4T**) and recently as substrates or inhibitors of the D-glutamate-adding enzyme[16] (**3E** and **4E**), this last enzyme belonging to the biosynthesis system of bacterial peptidoglycan.[17]

The aim of conformational analysis is to find all the thermally populated conformations of a molecule, *i.e.* the conformations with the lowest free energies, in order to provide important structural information on the properties of the

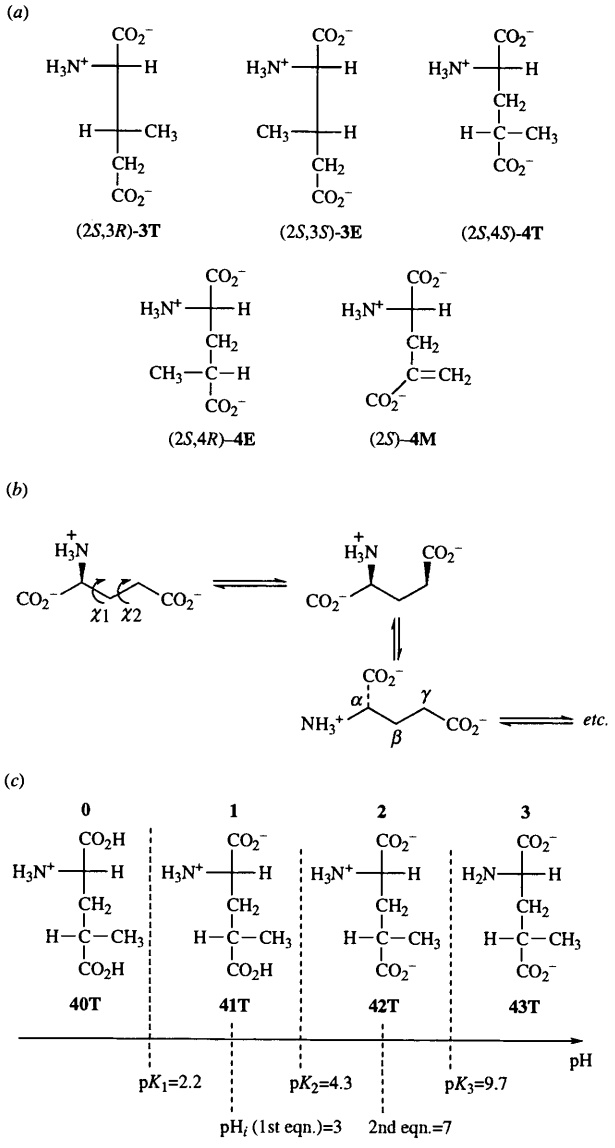

Fig. 1 (*a*) Structure of the five amino acid analogues studied in aqueous solution at pH 7: 3-methyl glutamic acid **3T** and **3E**, 4-methyl glutamic acid **4T** and **4E**, and 4-methylene glutamic acid **4M** (isomers α-*S* represented); (*b*) conformation of (L)-glutamic acid; (*c*) predominant forms of **4T** isomer in the different pH zones (from 0 to 3)

molecule. The modelling procedure used to generate the approximate ratios of low-energy conformers will also specify the structures representative of very hindered intermediates.

The practical methodologies employ molecular dynamics (MD) to generate conformations and include experimental analysis to determine the 3-D stucture from NMR data.

The advantage MD has in approaching thermodynamic equilibrium becomes a problem when searching for a particular high free energy conformation. For example, the conformation a molecule adopts after binding a receptor could be several kcal mol^{-1} higher in potential energy when calculated by itself than the energy of the global minimum. This will cause a problem if one tries to use MD searching for such receptor binding conformations, particulary if the ligands are ions or highly charged molecules, which is likely to have a large influence on their structures.

The receptor may be an acceptor or donor of protons. Hence, we have extended the NMR and the MD study in water at different pH values, so as not to neglect protonation effects which will induce particular conformations. It was interesting to examine the conformational changes induced by the electrostatic field generated by the different polarities of these molecules.

It is shown that by considering high resolution NMR and computerized molecular modelling, it is possible to obtain quantitative information about the populations and energy differences of rotational isomers in respect of the Cα–Cβ and Cβ–Cγ bonds of α-amino acid analogues in acid, neutral and alkaline solution. The experiments will provide useful information on the conformational behaviour of aqueous methylated glutamate using experimental values for the vicinal homo- and hetero-nuclear coupling constants, pH and temperature dependence of coupling constants and chemical shift data, and making use of theoretically calculated vicinal coupling constants on the relevant structures generated by MD. The methodology presented illustrates the usefulness of MD in elucidating possible solution conformations, and NMR data in revealing that approximate solution structures can be estimated.

Results and discussion

It is difficult to study the conformation of the linear methylated analogues[18] [Fig. 1(*a*)], because in these molecules there is a high degree of liberty around the C(2)–C(3) torsion angle χ1 and the C(3)–C(4) torsion angle χ2 [Fig. 1(*b*)]. The potential function for rotation about the C(2)–C(3) bond [or the C(3)–C(4) bond] shows that there exist three minimum energy conformations, or rotamers, in which the substituents on the two carbon atoms are 'staggered'. With typical barrier heights of the order of 3 to 12 kcal mol^{-1} according to the five molecules, the interconversion between the three rotamers relative to a single bond will be rapid or hindered. The stable forms of these α-amino acids are the three staggered configurations shown in [Fig. 2(*a*)] and the three others in [Fig. 2(*b*)], with the relative residence times '**A**, **B**, **C**' and '**a**, **b**, **c**', respectively. The C(2)–C(3)–C(4) system with two carbon–carbon single bonds allows the possibility of *trans* and *gauche* forms and there are a total of 3 × 3 = 9 rotamers, all of which are distinct. We obtain nine (or six) staggered conformations, resulting from the combination of the three rotamers '**A**, **B**, **C**' (rotation about χ1) with the three rotamers '**a**, **b**, **c**' or 'α, β' (rotation about χ2) (Fig. 2).

A conformational search on the zwitterionic molecules with ionized functional groups γ-CO_2^-, α-CO_2^- and α-NH_3^+ was performed at neutral pH. However, as three acidity functions are present in these compounds (pK_a = 2.2, 4.3 and 9.7) and the charges of the groups and their protonation depend on the pH of the solution, three predominant forms must be taken into account for the study in aqueous solution: **1** (pH 3), **2** (pH 7) and **3** (pH 10) [Fig. 1(*c*)]. The preferred conformation may depend on these charges because of the electrostatic interactions or hydrogen-bonding implied. At isoelectric pH (pHi = 3), the γ-carboxylate group is protonated and can provide a distal carboxylic acid which possesses a potential proton donor hydroxy group. At the opposite, pH = 10, the amino group carries no formal charge. We must then study each one of the 15 structures derived from the five compounds represented in [Fig. 1(*a*)]: the first number indicates the position of the methyl or methylene (at carbon **3** or **4**), the second one the predominant form in the pH zone considered (isoelectric zone **1**, neutral zone **2** and alkaline zone **3**) [Fig. 1(*c*)], the letter **E** or **T** the relative configuration of the methyl and **M** the methylene substituent. To every structure correspond nine (Aa, Ab, Ac, Ba, *etc.*) or six (Aα, Aβ, *etc.*) conformations characterized by the letter '**A**, **B**, **C**' for the rotamers about the torsion angle χ1 [Fig. 2(*a*)] and the letter '**a**, **b**, **c**' [Fig. 2(*b*)] or α, β [Fig. 2(*c*)] for the rotamer relative to the angle χ2.

In a certain sense then, one may regard MD generated structures as giving all the conformations available to the molecules. A large number of structures may be needed to get a complete picture. By contrast the NMR method as used for the –XCH–CHY-system in solution interprets the spectrum in

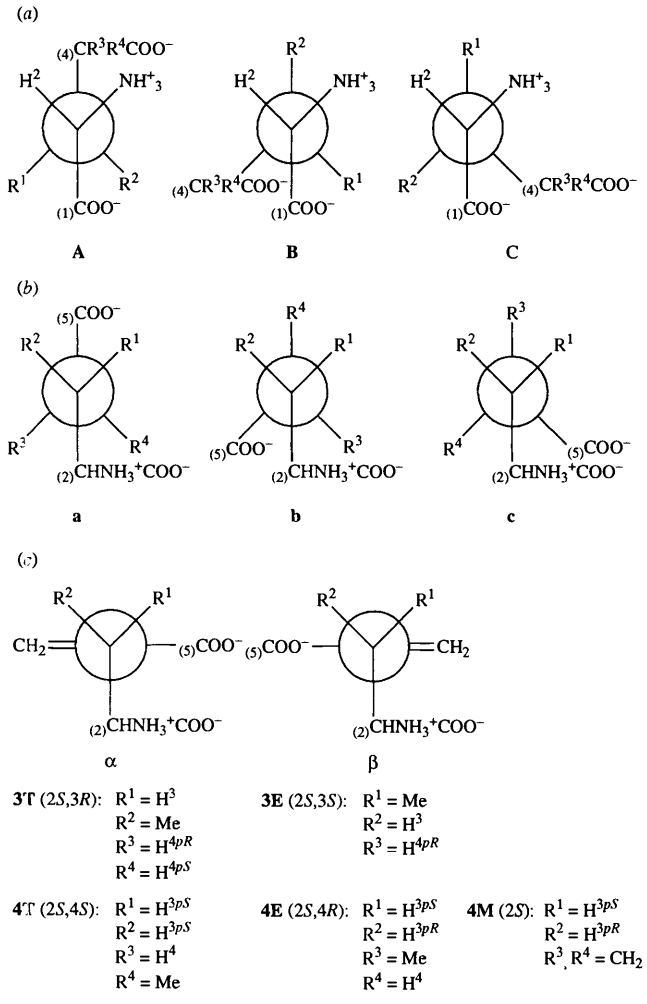

Fig. 2 Newmann projections for the three rotamers (*a*) '**A**, **B**, **C**' relative to the torsion angle $\chi 1$ [C(2)–C(3)], and (*b*) '**a**, **b**, **c**' or (*c*) 'α, β' relative to the $\chi 2$ angle [C(3)–C(4)]

terms of variable populations of staggered rotamers having dihedral angles of ±60 and 180°. The details of the NMR spectra and the methods of spectral analysis are reported here.

NMR spectroscopy

Assignments. For an unambiguous interpretation of the conformational NMR data, the complete assignment of the ^1H and ^{13}C NMR spectrum is an absolute prerequisite. The study was carried out on samples[19] dissolved in deuterium oxide and three pH values are considered: 3, 7 and 10, except for the carbon resonances which are examined only at pH 7 due to the solubility constraints and to the particular interest of this pH. The ^1H NMR spectrum at 500.13 MHz did not display spectral overlap and exhibited four spin systems. In all cases, the starting point was the signal of the 2-H proton, which has a higher resonance frequency than the other protons (because of the adjacent α-CO_2^- and α-NH_3^+ groups). In the ^{13}C NMR spectrum (125.76 MHz), it was clear that one-dimensional selective INEPT experiments[20] would be useful during the assignment procedures. With this experiment, based on a selective excitation of the 2-H proton, we could differentiate both α- and γ-carboxylate groups. However, less ambiguous is a correlation in the heteronuclear multiple bond correlation (HMBC) spectrum, in this case the correlation from 2-H to α-CO_2^-. The different isolated carboxylate groups of **4M** were only identified in the HMBC by their correlations *via* two-(2-H to α-CO_2^-) and three-bond (3a-H to α-CO_2^-; 3b-H to γ-CO_2^-; 6-H to γ-CO_2^-) couplings. The complete assignment of the ^1H (500.13 MHz) and ^{13}C NMR (125.76 MHz) signals of the five isomers was achieved at different pH values and is given in Table 1.

The assignment of the individual diastereotopic methylene protons was particularly difficult.[21] A simpler procedure is available as, in addition to the α-proton, there are other nuclei that will be coupled over three bonds to the β-protons, namely the α-carboxyl carbon (^{13}C) and the α-amino hydrogen (^{15}N). These ^{13}C–^1H and ^{15}N–^1H coupling constants are 'out of phase' with the ^1H–^1H coupling constants so that in rotamer **4T A** [Fig. 2(*a*)], for example, 3_{proS}-H and 3_{proR}-H are *gauche* and *trans*, respectively to 2-H, but are both *gauche* to the carboxyl carbon 1-C. One can use the $^3J_{^{13}C-^1H}$ (or $^3J_{^{15}N-^1H}$) coupling constants for this assignment.[21b] The experimental NMR data from 3-H are measured for **4T** at pH 7 (**42T**), $^3J_{2,3b}$ (4.8), $^3J_{2,3a}$ (8.9), $^3J_{C(1)H(3a)}$ (2.8) and $^3J_{C(1)H(3b)}$ (2.6) and thus, for **4T** the 3_{proR}-H is assigned to 3a-H and 3_{proS}-H to 3b-H. Hence, it was necessary to define the $^3J_{(C,H)}$ coupling constants[21d] of both diastereotopic protons and use these values in conjunction with the $^3J_{(H,H)}$ coupling constants to allow unambiguous assigments of the C(2)–C(3)–C(4) fragment (Table 2). For the different isomers, the most important coupling constants involve the C-atom of the methyl group of the 1- and 5-carboxylate groups (α or γ); their long-range couplings allow the assignment of the diastereotopic protons of the adjacent methylene group. The homonuclear and heteronuclear three-bond coupling constants of the five compounds, necessary for the assignments of the diastereotopic protons at C(3) and C(4), are listed in Table 2.

Coupling constants. Besides the assignments of the diastereotopic methylene protons, coupling constants were used to determine rotamer populations of dihedral angles. The conformational analysis is based on the $^3J_{^1H-^1H}$ and the $^3J_{^{13}C-^1H}$ coupling constants.

The experimental coupling constants associated with the orientation of the $\chi 1$ and $\chi 2$ torsion angles have been given in Table 2 (pH 7) and in Table S1† (pH 3 and 10). For the **3E**, **3T**, **4E** and **4M** isomers, the spin system is simpler because the protons are inequivalent at all pH values tested (Table 1). This allows a first-order analysis of the spin sub-system formed by 2-H, 3-H and 4-H to be made. The coupling constants are deduced from 1D spectra at 500 MHz and are confirmed by spectral simulation with the NMR II program. For the **4T** isomer, the spin system is complex because the two 3-H protons are nearly isochronous at the pH values 7 and 10 (Table 1). Coupling constants are not directly readable as the protons constituted a highly coupled system, 3a-H, 3b-H and 4-H, and the *J*- and δ-values are calculated by the sub-spectra method from 1D spectra at 500 MHz after irradiation of the 2-H proton. The second-order spectra analysis is confirmed by NMR simulation (NMR II program).

For the determination of heteronuclear coupling constants $^3J_{C,H}$ the relatively low concentration necessitated a sensitive method allowing good resolution. One method for the quantitative determination of heteronuclear coupling constants usually fulfills these demands: the 2D $J\delta$ selective INEPT[22] using polarization transfer from ^1H to ^{13}C, previously used in our laboratory, seems to be a good method available to measure couplings at quaternary C-atoms and others.

It is assumed that the NMR spectrum of such a molecular fragment [C(2)–C(3) or C(3)–C(4)] in a small molecule is the weighted average (weighted by the relative populations of the three rotamers '**A**, **B**, **C**' or '**a**, **b**, **c**', Fig. 2) of the spectra of each of the three rotamers. At neutral pH, the study was made at different temperatures (280, 290, 300 and 310 K) to permit a distinction between a fixed conformation and an average of two

† Tables S1–S4 are available as supplementary data (SUPPL. No. 57147) from the British Library. For details of the Supplementary Publications Scheme, see Instructions for Authors, *J. Chem. Soc., Perkin Trans. 1*, 1996, Issue 1.

Table 1 ^{1}H NMR chemical shifts in D_2O at various pH values ($\delta_H/[^2H_4]$TSP error 0.01 ppm) and ^{13}C NMR chemical shifts in D_2O at pH 7 ($\delta_C/[^2H_4]$TSP error 0.1 ppm), H noted a or b according to the stereospecificity of the proton

	3T[a]				**3E**[a]				**4T**[a]				**4E**[a]				**4M**[a]			
Molecular numbering	**31T**[b] pH 3	**33T**[b] pH 11	**32T**[b] pH 7	**32T**[c] pH 7	**31E**[b] pH 3	**33E**[b] pH 11	**32E**[b] pH 7	**32E**[c] pH 7	**41T**[b] pH 3	**43T**[b] pH 11	**42T**[b] pH 7	**42T**[c] pH 7	**41E**[b] pH 3	**43E**[b] pH 11	**42E**[b] pH 7	**42E**[c] pH 7	**41M**[b] pH 3	**43M**[b] pH 11	**42M**[b] pH 7	**42M**[c] pH 7
1				176.8				176.7				178.0				177.7				176.9
2	3.76	3.21	3.75	61.9	3.80	3.09	3.71	62.0	3.74	3.24	3.67	56.6	3.76	3.23	3.76	56.1	3.98	3.40	3.89	57.4
3a	2.56	2.30	2.55	34.5	2.52	2.09	2.47	34.5	2.10	1.71	1.99	38.3	2.17	1.93	2.13	37.4	2.97	2.77	2.92	37.2
b									1.95	1.68	1.94		1.89	1.50	1.89		2.77	2.36	2.69	
3Me	1.02	0.85	1.02	16.8	1.05	0.93	1.07	17.8												
4a	2.49	2.35	2.44	44.5	2.60	2.37	2.41	43.6	2.67	2.39	2.48	42.9	2.56	2.39	2.47	42.0				143.6
b	2.32	2.04	2.26		2.40	1.91	2.23													
4Me									1.22	1.10	1.17	20.4	1.19	1.11	1.17	20.7				
5				183.5				183.5				187.5				187.5				178.2
6a																	6.36	5.84	5.97	128.4
b																	5.88	5.41	5.55	

[a] The first number indicates the position of the methyl or methylene (at carbon **3** or **4**), the second the predominant form in the pH zone considered (isoelectric zone **1**, neutral zone **2** and alkaline zone **3**), the letter **E** or **T** the relative configuration of the methyl and **M** the methylene substituent. [b] ^{1}H. [c] ^{13}C.

Table 2 Homonuclear (^{1}H, ^{1}H) and heteronuclear (^{13}C, ^{1}H) coupling constants in D_2O (Hz, error ± 0.3 Hz) used in the conformational analysis of the five isomers (**3T**, **3E**, **4T**, **4E**, **4M**) and for the assignment of the diastereotopic methylene protons at C(3) or C(4)

	J/Hz			J/Hz			J/Hz
Coupling	**3T**[a]	**3E**[b]	Coupling	**4T**[c]	**4E**[d]	Coupling	**4M**[c]
^{1}H, ^{1}H			^{1}H, ^{1}H			^{1}H, ^{1}H	
2, 3	3.5	4.0	2, 3a	8.9	4.5	2, 3a	3.7
3, 4a	5.2	4.6	2, 3b	4.8	8.2	2, 3b	8.3
3, 4b	7.8	8.3	3a, 4	7.3	8.8		
			3b, 4	7.3	5.2		
^{1}H, ^{13}C			^{1}H, ^{13}C			^{1}H, ^{13}C	
4a-H, 2-C	3.9	4.3	4-H, 2-C	2.7	3.2	2-H, 4-C	4.8
4a-H, 3Me-C	5.2	4.6	2-H, 4-C	3.3	4.1	3a-H, 1-C	4.4
4b-H, 2-C	3.0	2.7	3a-H, 1-C	2.8	3.9	3a-H, 5-C	5.7
4b-H, 3Me-C	5.0	4.6	3a-H, 5-C	2.0	3.5	3a-H, 6-C	3.3
2-H, 4-C	3.3	4.7	3a-H, 4Me-C	4.2	3.4	3b-H, 1-C	1.5
2-H, 3Me-C	5.4	3.6	3b-H, 1-C	2.6	2.5	3b-H, 5-C	5.2
3-H, 5-C	—	<2	3b-H, 5-C	5.0	6.0	3b-H, 6-C	5.2
3-H, 1-C	—	3.2	3b-H, 4Me-C	3.7	3.5		

[a] 4a-H, *pro R*; 4b-H, *pro S*. [b] 4a-H, *pro S*; 4b-H, *pro R*. [c] 3a-H, *pro R*; 3b-H, *pro S*. [d] 3a-H, *pro S*; 3b-H, *pro R*.

or more conformations. The observed coupling constants do not change appreciably as the temperature increases. It is, however, usually not practical, especially in aqueous solutions of small molecules, to lower the temperature far enough to prove the existence of averaging and to characterize the individual conformers by 'freezing out'. A distinction between fixed and averaged conformations is also possible by making use of the fact that the dihedral angles about the C(2)–C(3) bond governing the coupling to the two 3-H protons [or 4 H, in the C(3)–C(4) fragment] must differ by 120°. For example, it appears for **4T** that the two coupling constants between the 2- and 3-H of 8.9 and 4.8 Hz could not be produced by any pair of values of $\chi 1$ differing by 120° (using the Karplus equation shown below, with appropriate values for the constants). All the observed pairs of proton–proton (and the corresponding ^{1}H–^{13}C) coupling constants in Table 2 are consistent with averaged coupling constants.

In the C(2)–C(3) fragment, the 2-H and 3-H protons [or 3-H and 4-H, in the C(3)–C(4) fragment] are either *gauche* or *trans* and the coupling constants corresponding to these two arrangements are denoted J_g and J_t, respectively (the same for the two vicinal atoms ^{1}H–^{13}C). The average coupling constant observed for the two individual 3-H (or 4-H) protons will then be for **4T**, for example, as in eqns. (1) and (2), where the P_A, P_B

$$^3J_{2,3a} = P_AJ_t + P_BJ_g + P_CJ_g \qquad ^3J_{4,3a} = P_aJ_g + P_bJ_t + P_cJ_g \quad (1)$$

$$^3J_{C(1)H(3a)} = P_AJ_g + P_BJ_t + P_CJ_g \qquad ^3J_{C(5)H(3a)} = P_aJ_g + P_bJ_g + P_cJ_t \quad (2)$$

and P_C (or P_a, P_b and P_c) are the fractional populations of the three rotamers, according to eqn. (3).

$$P_A + P_B + P_C = 1 \qquad P_a + P_b + P_c = 1 \quad (3)$$

Equations (1)–(3) can be solved for P_A, P_B and P_C (or P_a, P_b and P_c), provided that appropriate values of J_g and J_t are known. The ^{1}H–^{1}H coupling constants will, like ^{13}C–^{1}H coupling constants, vary with the dihedral angles about the C(2)–C(3) and C(3)–C(4) bonds and with the electronegativity of the substituents according to the Karplus relationship [eqn. (4)],[23] with coefficients in the homonuclear case[24] A = 9.5, B = −1.3 and C = 1.6 and in the heteronuclear case[25]

$$^3J = A\cos^2\varphi + B\cos\varphi + C \quad (4)$$

A = 5.7, B = −0.6 and C = 0.5, and will thus be related to the rotamer populations by equations analogous to eqns. (1)–(3).

For an analysis in terms of rotamer populations, values of J_g and J_t are required. The most widely used values are those proposed by Pachler:[26] J_g = 2.60 Hz, J_t = 13.56 Hz, for $^3J_{HH}$ [for comparison, eqn. (4) gives, approximately: J_g = 3.3 Hz, J_t = 12.4 Hz, for $^3J_{HH}$ and J_g = 1.8 Hz, J_t = 6.5 Hz, for $^3J_{HC}$]. In what follows, we will calculate the theoretical values of these conformationally informative coupling constants of torsion angles computed by MD for **3T**, **3E**, **4T**, **4E** and **4M**, using Karplus type-equations. Values of J_g and J_t, coupling constants ($^3J_{^1H-^1H}$ and $^3J_{^{13}C-^1H}$ for vicinal atoms of a H–C–C–H or a H–C–C–C segment) will thus differ in different rotamers. Reasonable values of J_g and J_t for the different rotamers are given in Table 3. None of the three rotamers alone can reproduce the experimental values for **3E**, **3T**, **4E**, **4T** and **4M**, and averaging between a population of rotamers has to be considered.

When assuming that the $\chi 1$ and $\chi 2$ torsion angles are restricted to the three staggered population **A**, **B** and **C** or **a**, **b** and **c**, (even though MD suggests some 'eclipsed' or less-staggered rotamers which represent high-energy intermediates neighbouring to the transition state) and using the J_t and J_g couplings values calculated in Table 3, it is possible to calculate their population distributions (Table 4). This result is supported by many independent determinations of homonuclear and heteronuclear coupling constants about the C(2)–C(3) ($\chi 1$) and C(3)–C(4) ($\chi 2$) bonds [$^3J_{H(2)H(3)}$, $^3J_{C(4)H(2)}$, $^3J_{C(Me)H(2)}$, $^3J_{C(1)H(3)}$ and $^3J_{H(3)H(4)}$, $^3J_{C(2)H(4)}$, $^3J_{C(5)H(3)}$ and $^3J_{C(Me)H(3\text{ or }4)}$, respectively].

The error in calculating the population of staggered rotamers is due to inaccuracies in the assumed values for the J_t and J_g coupling constants. The error in fractional populations is also dependent on the magnitude of the measured coupling constant (0.2 and 0.3 Hz). It appears that rotamer populations accurate to ± 10% can still be obtained.

Thus, the experimentally determined coupling constants $^3J_{^1H-^1H}$ and $^3J_{^{13}C-^1H}$ presented in Table 2 allow us to determine with tolerable precision the mole fractions for each rotamer—P_A, P_B and P_C or P_a, P_b and P_c. Considering the rotamer distribution for the glutamic acid analogues **3E**, **3T**, **4E**, **4T** and **4M**, the major species in aqueous solution are **A** and **c** for **32T**, **C** and **b** for **32E**, **A** and **b** for **42T**, **A** and **c** for **42E** and **B** and

Table 3 Torsion angles and coupling constants[a] (^3J/Hz) computed for **3T**, **3E**, **4T**, **4E** and **4M** from the different conformations generated by MD at neutral pH

	Torsion angle (°) (and ^3J/Hz)							Torsion angle (°) (and ^3J/Hz)								
	3T			**3E**				**4T**			**4E**			**4M**		
$\chi1$	**A**	**B**	**C**	**A**	**B**	**C**	$\chi1$	**A**	**B**	**C**	**A**	**B**	**C**	**A**	**B**	**C**
2, 3	−63.6	175.9	58.1	174.0	66.0	68.4	2, 3*pR*	175.6	73.4	−50.6	171.5	77.3	−55.8	173.3	73.8	−62.2
	(2.9)	(12.3)	(3.6)	(12.3)	(2.6)	(2.4)		(12.3)	(2.0)	(4.6)	(12.2)	(1.8)	(3.9)	(12.2)	(2.0)	(3.1)
2-H, 4-C	51.4	−56.9	176	61.5	−45.8	172.3	2, 3*pS*	−71.6	173.2	61.1	−69.0	168.8	54.1	−66.8	173.1	47.8
	(2.3)	(1.9)	(6.8)	(1.5)	(2.8)	(6.7)		(2.1)	(12.3)	(3.2)	(2.3)	(12.0)	(4.1)	(2.6)	(12.2)	(5.0)
2-H, 3Me-C	175.5	66.1	−56.5	−61.2	174.7	44.5	2-H, 4-C	49.5	−50.4	171.8	52.3	−44.2	175.4	54.9	−46.9	171.7
	(6.8)	(1.2)	(1.9)	(1.5)	(6.7)	(3.0)		(2.5)	(2.4)	(6.7)	(2.3)	(3.0)	(6.8)	(2.0)	(2.7)	(6.7)
							3*pR*, 1-C	−61.7	156.4	−67.9	−64.3	160.6	58.2	−61.2	164.7	53.9
								(1.5)	(5.8)	(1.1)	(1.3)	(6.1)	(1.8)	(1.5)	(6.4)	(2.1)
							3*pS*, 1-C	−51.1	42.6	177.3	48.7	−46.9	168.8	−51.5	−51.6	164.0
								(2.4)	(3.1)	(6.8)	(2.6)	(2.7)	(6.6)	(2.3)	(2.3)	(6.3)

$\chi2$	**a**	**b**	**c**	**a**	**b**	**c**	$\chi2$	**a**	**b**	**c**	**a**	**b**	**c**	α	β
3, 4*pS*	73.9	−53.8	170.7	170.8	68.3	−55.8	3*pR*, 4	−68.5	174.8	55.2	175.9	63.4	−67.6		
	(2.0)	(4.1)	(12.1)	(12.1)	(2.4)	(3.9)		(2.4)	(12.3)	(3.9)	(12.4)	(2.9)	(2.5)		
3, 4*pR*	170.6	60.3	−70.0	−73.6	176.9	56.6	3*pS*, 4	175.2	76.6	−56.2	−69.6	46.7	173.7		
	(12.1)	(3.3)	(2.3)	(2.0)	(12.4)	(3.8)		(12.3)	(1.8)	(3.8)	(2.3)	(5.2)	(12.3)		
4*pR*, 2-C	72.3	−55.0	167.7	−43.5	54.5	171	4-H, 2-C	−53.1	55.2	175.5	−52.0	170.9	52.7		
	(0.8)	(2.0)	(6.5)	(3.1)	(2.1)	(6.6)		(2.2)	(2.0)	(6.8)	(2.3)	(6.6)	(2.2)		
4*pS*, 2-C	−43.2	169.4	50.2	72.0	169.6	−60.6	3*pR*, 5-C	47.2	−58.6	172.3	71.8	−54.9	170.5	147.2	35.2
	(3.1)	(6.6)	(2.4)	(0.9)	(6.6)	(1.6)		(2.7)	(1.7)	(6.7)	(0.9)	(2.0)	(6.6)	(5.0)	(3.8)
4*pR*, 3Me-C	−53.9	174.2	48.4	169.9	−71.5	56.1	3*pS*, 5-C	−66.3	171.5	65.1	−41.0	166.7	58.7	34.9	147.4
	(2.1)	(6.7)	(2.6)	(6.6)	(0.9)	(1.9)		(1.2)	(6.7)	(1.3)	(3.3)	(6.5)	(1.7)	(3.8)	(5.0)
4*pS*, 3Me-C	169.5	60.1	−71.4	−54.4	43.5	168.4	3*pR*, 3Me-C	169.8	64.6	−56.3	−51.6	174.8	47.9	33.8	146.4
	(6.6)	(1.6)	(0.9)	(2.1)	(3.1)	(6.6)		(6.6)	(1.3)	(1.9)	(2.3)	(6.4)	(2.6)	(3.9)	(4.9)
							3*pS*, 3Me-C	−57.1	48.3	167.0	164.4	−63.6	65.0	146.1	34.2
								(1.9)	(2.6)	(6.5)	(6.4)	(1.4)	(1.3)	(4.9)	(3.9)

[a] The coupling constants values $^3J_{HH}$ and $^3J_{HC}$ were calculated by using Karplus type-equations (ref. 23): $^3J = A\cos^2\varphi + B\cos\varphi + C$ with different coefficients in the homonuclear case (ref. 24) ($^3J_{HH}$) $A = 9.5$, $B = -1.3$ and $C = 1.6$ and in the heteronuclear case (ref. 25) ($^3J_{HC}$) $A = 5.7$, $B = -0.6$ and $C = 0.5$.

Table 4 Populations of rotamers[a] about $\chi 1$ and $\chi 2$

Rotamer	3T	3E	4T	4E	4M
A	**72**	15	**65**	**55**	10
B	5	30	20	20	**60**
C	23	**55**	15	25	30
a	27	20	35	20	
b	23	**55**	**50**	25	
c	**50**	25	15	**55**	
α					**75**
β					25

[a] The major populations of rotamers about $\chi 1$ and $\chi 2$ are shown in bold.

α for **42M**. Furthermore, these data will be confirmed in the molecular modelling work.

For the amino acids **3T**, **4E** and **4T**, the dominant conformation related to the $\chi 1$ dihedral angle is the fully extended rotamer **A** [α-CO_2^-–C(2)–C(3)–C(4)] where the side-chain substituent is *trans* to the α-CO_2^- group. Only **4T** and **3E** have a significant probability of adopting the 'folded' α-NH_3^+–γ·CO_2^- conformation **b** related to the $\chi 2$ torsion angle in the *gauche* form about [$^+$NC(2)–C(3)–C(4)–γCO_2^-].

At pH 3 (Table S1 of supplementary material), when the 3-carboxy group and the 1-amino group are protonated, the couplings corresponding to the first torsion angle $\chi 1$ and the second torsion angle $\chi 2$ show that an equilibrium still occurs for the five analogues, but not with the same proportions. The protonation effect may be an evident influence in stabilizing, in addition, new conformations of rotamers: **A** and **c** for **31T**, **C** and **b** for **31E** and **B** and **b** for **41T**.

At alkaline pH (Table S1 of supplementary material), the population of the rotamer '**A**' increases about $\chi 1$ and the rotamer '**a**' relative to $\chi 2$ is now the major one where the side-chain is *trans* to the α- and γ-CO_2^- groups. At pH 10, the preferred **4T** conformation is the sterically favoured one '**A**' (for $\chi 1$) or '**a**' (for $\chi 2$) while at intermediate pH (3 and 7) the '**A**, **B** and **b**' conformers are very likely stabilized by an electrostatic interaction (such as a hydrogen bond) between the 1-ammonium and the 3-carboxylate or between the 1-carboxylate and the 3-carboxy groups.

It is important to compare the NMR results (Table 2) to those obtained from molecular modelling (Tables 3, 5 and 6) in order to identify the corresponding solution conformations and to check if the rotamers estimated in the different solutions correspond to the approximate ratios of low-energy conformers generated by the modelling procedure.

Molecular modelling

Molecular mechanics. The nine different conformations of the **3T**, **3E**, **4T**, **4E** and **4M** isomers are minimized by molecular mechanics (Table S2 of supplementary material). Using the Boltzmann distribution, the relative population of each conformer is given by the eqn. (5). A widely used method to

$$P_i = \exp(-E_i/kT)/\Sigma\exp(-E_i/kT) \qquad (5)$$

mimic the solvent screening effect is to use a distance-dependent relative permittivity $\varepsilon = r^2$.[27] Upon direct minimization with $\varepsilon = 5$,[28] an electrostatic attraction between the α-NH_3^+ and the γ-CO_2^- groups leads to the lowest energy structure Ab, in the case of the five isomers, but this is not entirely consistent with the NMR results. So, if we reduce the electrostatic contribution by using $\varepsilon = 78$, the agreement between the corresponding populations of rotamers and the NMR experimental data (Tables 4 and 6) is improving but is not perfect. Minimization by molecular mechanics in a solvent box with the introduction of explicit water molecules in order to reduce the electrostatic contribution is not of practical use, as the energies of the corresponding minimized molecules, and thus their relative populations, are very difficult to evaluate (the energies obtained in Table S2 of supplementary material are those of 'molecule + 18 H_2O' systems).

This result indicates that ranking the conformations according only to their potential energies could be misleading in certain cases.

Molecular dynamics. For these charged, flexible methylated molecules, it is obvious that other methods may have to be used in a MD study, to obtain a more reasonable stastistical participation of every structure. The results are summarized in Figs. 3–5 and in Tables 3, 5 and 6.

Temperature.—For a preliminary exploration of the conformational space, we performed a MD run for the nine conformations of each compound at 300 K with periodic temperature jumps to 600 K. Conformational searches are often performed at high temperature as the large amount of kinetic energy present allows high potential energy barriers separating interesting regions of conformational space to be crossed (Table S3 of supplementary material).[29] The results cannot lead to a statistical evaluation of the different conformations which participate in the NMR solution because temperature is an important factor. If the temperature increases, this allows conformational changes to take place on the time scale of molecular dynamics simulations. At high temperature the molecule explores more states; however, the fraction of time it spends near the lowest energy states is smaller.

In the case of **4T** the relative energy-difference between the lowest energy-minimized structure **Ab** and the highest one **Cb** is approximately 12 kcal mol^{-1}.† If one examines the transformation of the **4T** molecule (Fig. 5) which occurred in the solvation box during the MD experiments (300 K with jumps to 600 K), one observes that the presence of water molecules favoured, during the trajectory, some 'less-staggered' rotamers which represent high-energy intermediates close to a particular transition state implied in the rotational conversion (*i.e.* **C**→**C***→**A**→**A***→**B**). The high-energy intermediates are almost in an 'eclipsed' form (represented by the symbol*) with a ±80–90° *gauche* torsion angle instead of ±60° according to the staggered rotors $\chi 1$ and $\chi 2$ [Fig. 5(*a*)]. The MD run from **4T** **Ab** leads to another low-energy structure **Ab** [Fig. 5(*b*)]. This transition occurs through four **Ab*** structures (*i.e.* with a 90° *gauche* torsion angle '**b**' instead of the 65° staggered rotor) but does not allow an interconversion of the corresponding rotamers to take place.

This allows us to conclude that high rotational barriers have to be passed for the **4T** isomer to observe the rotational conversion, since an important electrostatic (the α-NH_3^+ and the γ-CO_2^- groups) and steric contribution in **4T** leads to a very good stabilization of the Ab conformation and hinders an interconversion of the corresponding rotamers [Fig. 5(*b*)].

These constrained structures, which represent high-energy intermediates neighbouring to the transition state, are observed with the four isomers **3E**–**4T** in an aqueous environment.

Dielectric constant.—After having considered various MD protocols, the most accurate way of including an environment is to explicitly include the solvent atoms themselves. This is, of course, more expensive computationally. The effective electrostatic interaction between two charged end-groups of a molecule will be reduced as water molecules will arrange themselves so as to effectively screen the interaction. If the solvent molecules are explicitly included in the simulation, then this effect will already be taken into account, and the dielectric constant assigned should be close to one. We have constructed solvation boxes containing 48 water molecules using boundary conditions, and MD experiments were carried out at neutral pH on the zwitterionic molecules with ionized functional groups

† 1 cal = 4.184 J.

Table 5 Simulations[a] for the nine conformations of the **4T** isomer at pH 7 (**42T**). Each column represents one simulation, '×' indicates that conformation was found and in brackets (frequency). Frequency is the number of times each conformation was found

Final conformation	Starting conformations									Total frequency	Percentage (%)
	Aa	**Ab**	**Ac**	**Ba**	**Bb**	**Bc**	**Ca**	**Cb**	**Cc**		
Aa								× (100)		100	11
Ab	× (100)	× (100)			× (100)	× (100)	× (100)			500	56
Ac			× (100)							100	11
Ba				× (100)						100	11
Bb										0	0
Bc										0	0
Ca										0	0
Cb										0	0
Cc									× (100)	100	11

[a] 100 ps simulations at 300 K in a water box ($\varepsilon = 1$). The same format of table was performed for **3T**, **3E**, **4T**, **4E** and **4M** at different pH values. The percentage of each conformation deduced from their frequency is reported in Table 6.

Table 6 Results of the MD simulations with the percentage of each conformation (**Aa**, **Ab**, *etc.*) and each rotamer[c] (**A**, **B**, *etc.*) generated, starting from the nine conformations of each isomer

	3T[a]	**3E**[b]	**4T**[a]	**4E**[a]		**4M**[a]
Aa	11	11	11	0	**Aα**	5
Ab	34	0	56	34	**Aβ**	16
Ac	22	11	11	22	**Bα**	60
Ba	11	0	11	22	**Bβ**	0
Bb	0	23	0	0	**Cα**	8
Bc	0	11	0	0	**Cβ**	11
Ca	0	11	0	0		
Cb	0	22	0	0		
Cc	22	11	11	22		
A	67	22	78	56	**A**	21
B	11	34	11	22	**B**	60
C	22	44	11	22	**C**	19
a	22	22	22	22	α	73
b	34	45	56	34	β	27
c	44	33	22	44		

[a] The MD simulations was performed at neutral pH on the zwitterionic molecules with ionized functional groups γ-CO_2^-, α-CO_2^- and α-NH_3^+ during 100 ps at 300 K in a water box ($\varepsilon = 1$). [b] The MD simulations was performed at isoelectric pH with ionized functional groups γ-CO_2H, α-CO_2^- and α-NH_3^+ during 200 ps at 300 K ($\varepsilon = 5$) (ref. 28). [c] An ensemble of nine separate trajectories of 100 or 200 ps starting from nine separate staggered conformations was calculated for a reliable statistical convergence and we have reported populations of rotamers (%) about $\chi 1$ and $\chi 2$ from the percentage of each conformations generated with these protocol (for each isomer 900 or 1800 structures were examined).

γ-CO_2^-, α-CO_2^- and α-NH_3^+. All subsequent protocols are based on the 300 K, 48 H_2O, $\varepsilon = 1$ protocol which seems to be the generally appropriate experiment for **3T**, **4T**, **4E** and **4M** since good agreement is observed with the NMR results (Table 6, Fig. 6).

The less good correspondence for **3E** indicates a difficult compromise between the steric effects and any intramolecular stabilizing forces, and thus suggests a relative modification of the force field. So, if we reduce the electrostatic contribution on **3E** by removing one formal charge (*i.e.* on the γ-carboxylate group), we conceive a protocol on **3E** at isoelectric pH (**31E**) with functional groups γ-CO_2H, α-CO_2^- and α-NH_3^+ during 200 ps at 300 K ($\varepsilon = 5$),[28] The **Bb** and **Cb** conformations are now favoured and the calculated populations of rotamers are then in a better agreement with the NMR experimental data, for this isomer (Table 6, Fig. 6).

Sampling time.—To find an optimal protocol for better sampling and statistical evaluation, another factor has to be considered, the time of MD run. This should be sufficient to sample all of the conformational space. The minor difference tested between multiple long MD runs (100 ps) and one very long MD (2 ns) had encouraged us to use the method of multiple starting points[30] in order to better sample phase space. Of course, one could postulate that this method helps to improve the result, but choosing the starting structures is likely to be crucial there. It is not a difficulty here, since MD runs were achieved for the nine possible minimized conformations of each isomer. The nine minimized conformations (**Aa**–**Cc**) were then used as the starting structures of each isomer, for a 100 ps MD run. A time of 100 ps is sufficiently long to provide much physical insight into the systems of interest.[29,31] The frequency (how many times we get the same conformation) deduced from the different structures is reported in Table 5.

For these studied amino-acids a range of conformations is clearly available to the molecules in solution, and no one conformation is exclusively favoured. The structures found to have ratios up to 10% (Fig. 3) will be considered representative of the different NMR solutions (Table 6).

Surprisingly, one notices for **4T** (Table 5) that from major starting structures, only the **Ab** conformation is generated stabilized by the electrostatic interaction between γ-CO_2^- and α-NH_3^+, in spite of hydration; this result, which is in agreement with **4T** NMR data, may be explained since MD reveals that any water molecules are located between the two charged groups. The distance between the two opposite charges is very small (≤ 3 Å) and water molecules surround both charges at the same time rather than each charge separately.

In Table 5, one can see the structures which have a very high sampling probability and thus should have a very low relative free energy in the presence of water. For example, the 900 minimized structures of one isomer **4T** lead to 500 structures of the previous lower energy **Ab** conformation (56%) and to the same percentage (11%) of **Aa**, **Ac**, **Ba** and **Cc**.

From the various solutions resulting from the MD approach (Table S3 of supplementary material), one set for each isomer presented good agreement (Table 6) with the populations of rotamers obtained from NMR spectra, *i.e.* vicinal $^3J_{^1H,^1H}$ coupling constants and especially, long-range heteronuclear $^3J_{^{13}C,^1H}$ coupling constants (Table 2). The protocol with the presence of water molecules seems to be generally the appropriate experiment for **3T**–**4M**, since good agreement is observed with the NMR results (Fig. 6). A less good agreement characterizes a difficult compromise between the intermolecular forces such as hydrogen-bonding possibilities, steric effects and any intramolecular stabilizing forces. If one surveys the C(2)–C(3) dihedral angle in the variety of studied molecules with these particular groups (α-CO_2^-, γ-CO_2^-, α-NH_3 and CH_3), one observes a wide range of *trans*-orientations about this torsion angle. The '**A**' orientation [α-CO_2^-–C(2)–C(3)–C(4)] (170°) is observed in the NMR structures of **3T**, **4T** and **4E** while the '**C**' orientation of the angle [α-CO_2^-–C(2)–C(3)–C(Me)] (170°) is favoured by a different steric interaction in the **3E** structure. In **4M** solution where the double-bond character

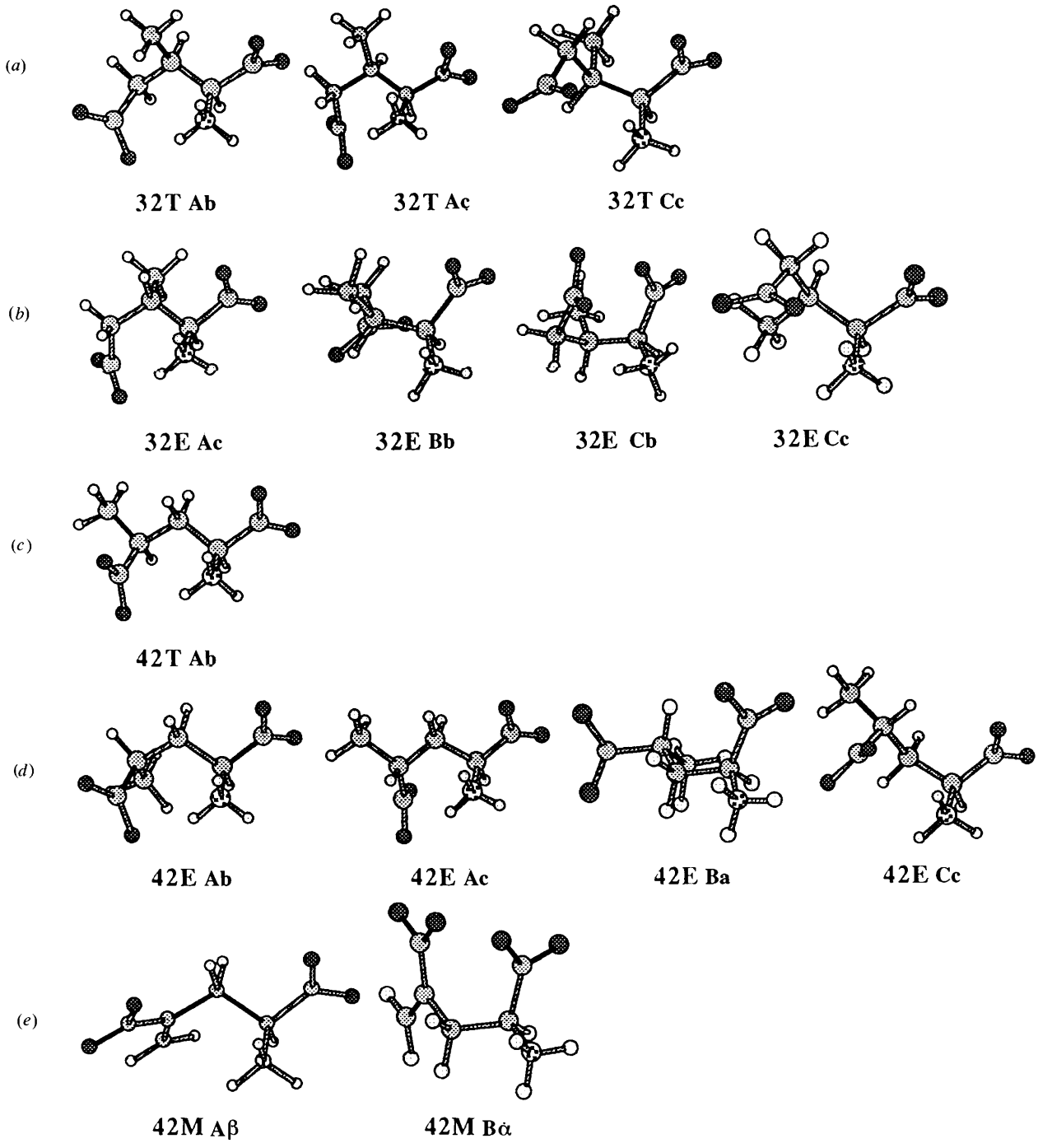

Fig. 3 Achieved major conformations at neutral pH for the amino acid analogues **3T**, **3E**, **4E**, **4T** and **4M**: (*a*) the three conformations of **32T**: **Ab**, **Ac** and **Cc**; (*b*) the four conformations of **32E**: **Ac**, **Bb**, **Cb** and **Cc**; (*c*) the conformation of **42T**: **Ab**; (*d*) the four conformations of **42E**: **Ab**, **Ac**, **Ba** and **Cc** and (*e*) the two conformations of **42M**: **Aβ** and **Bα**

of the methylene moiety ensures a planar group, theoretical and solution results agree with the '**B**' orientation [α-NH_3^-–C(2)–C(3)–C(4)] (170°), despite intramolecular forces not being well-defined. Change of the first torsion angle $\chi 1$ is caused by the coulumbic expression (or a different steric contribution) and a specific conformation of the C(2)–C(3) angle is observed according to the different structures.

These derivatives exist as different ions or highly charged molecules and thus in order not to neglect the protonation effect, this study also extends to different pH values (Table S3 of supplementary material) to use MD searching for the particular induced conformations. At pH 3 and 10, the electrostatic interactions are sufficiently reduced and the conformations of **3E** and **4E** are the sterically favoured ones (Fig. 4). For **4T**, when the γ-CO_2^- carboxylate group is protonated, an interaction (like a hydrogen bond) is established with the α-CO_2^- and some conformers which were minor at pH 7 are now favoured, such as **41T Bb**. All the conformations observed at acidic pH presented two planes at 180° relative to each other for the γ-CO_2H group and thus the hydroxy group presents two different topologies. At alkaline pH, the '**a**' conformer with the two carboxylate groups 'extended' is predominant. The preferred conformation of the unprotonated molecule is the sterically favoured one: for example, **43T Aa** showing a large zig-zag alkylamine chain ending in a carboxylate group, or **43E Ba**, corresponding to a large 'W' between the amino and the carboxylate groups. The predominant conformations at different pH values (Figs. 3 and 4) are in agreement with the experimental NMR data (Table S1 of supplementary material).

An important result of this study is the agreement between the most significant conformers (percentage ≥15) determined

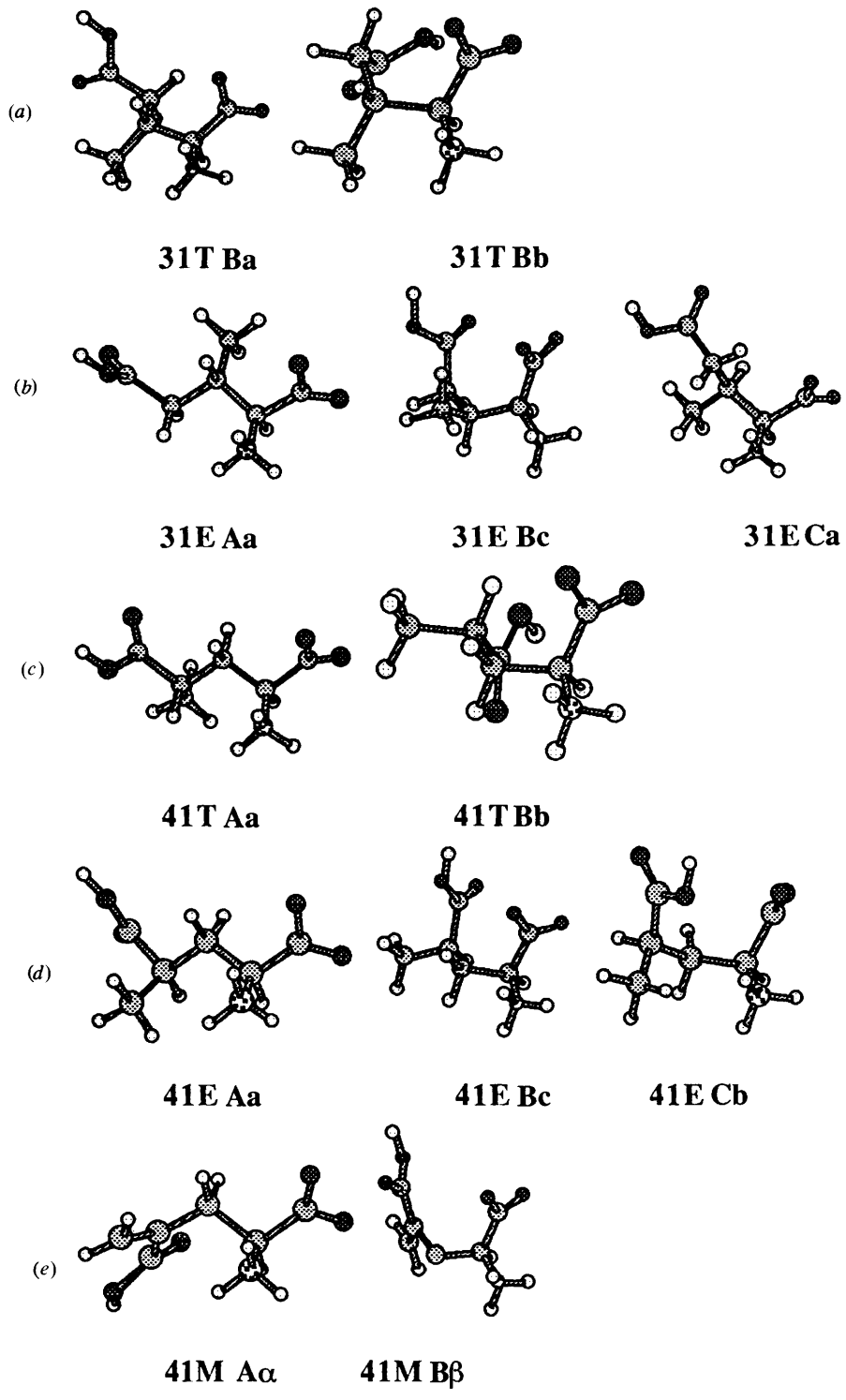

Fig. 4 Achieved major conformations at isoelectric pH (pH 3) for the amino acid analogues **3T**, **3E**, **4E** and **4M**: (*a*) the two conformations of **31T**: **Ba** and **Bb**; (*b*) the three conformations of **31E**: **Aa**, **Bc** and **Ca**; (*c*) the two conformations of **41T**: **Aa** and **Bb**; (*d*) the three conformations of **41E**: **Aa**, **Bc** and **Cb** and (*e*) the two conformations of **41M**: **A**α and **B**β. [The first number indicates the position of the methyl or methylene (at carbon **3** or **4**), the second one the predominant form in the pH zone considered (isoelectric zone **1**, neutral zone **2** and alkaline zone **3**), the letter **E** or **T** the relative configuration of the methyl and **M** the methylene substituent.]

from the theoretical MD structures and the preponderant experimental NMR results in solution (Fig. 6). NMR parameters reflect the virtual conformation and at the same time the MD experiments are of great benefit in predicting the specific range of conformations available to each derivative in solution.

Structural characteristics. The superimposition of C(1) and the central atoms of the two functional groups, *i.e.* the α-N and α-C(α-CO_2^-) of the different conformers deduced from the NMR and MD data of the five analogues, presents several conformational similarities and thus corresponding families. Conformational similarities of the five studied compounds were evaluated by calculating the root mean square (RMS) deviation between heavy atoms after superimposition. The results represent groups of structures whose small RMS deviations (< 0.6 Å) suggested that they may belong to the same conformational family (Table S4 of supplementary material). The differentiation of these families is due to electrostatic attraction or repulsion, along with the steric hindrance.

The conformational and the electrostatic energy terms were generally the most significant classification criteria from a physical point of view.

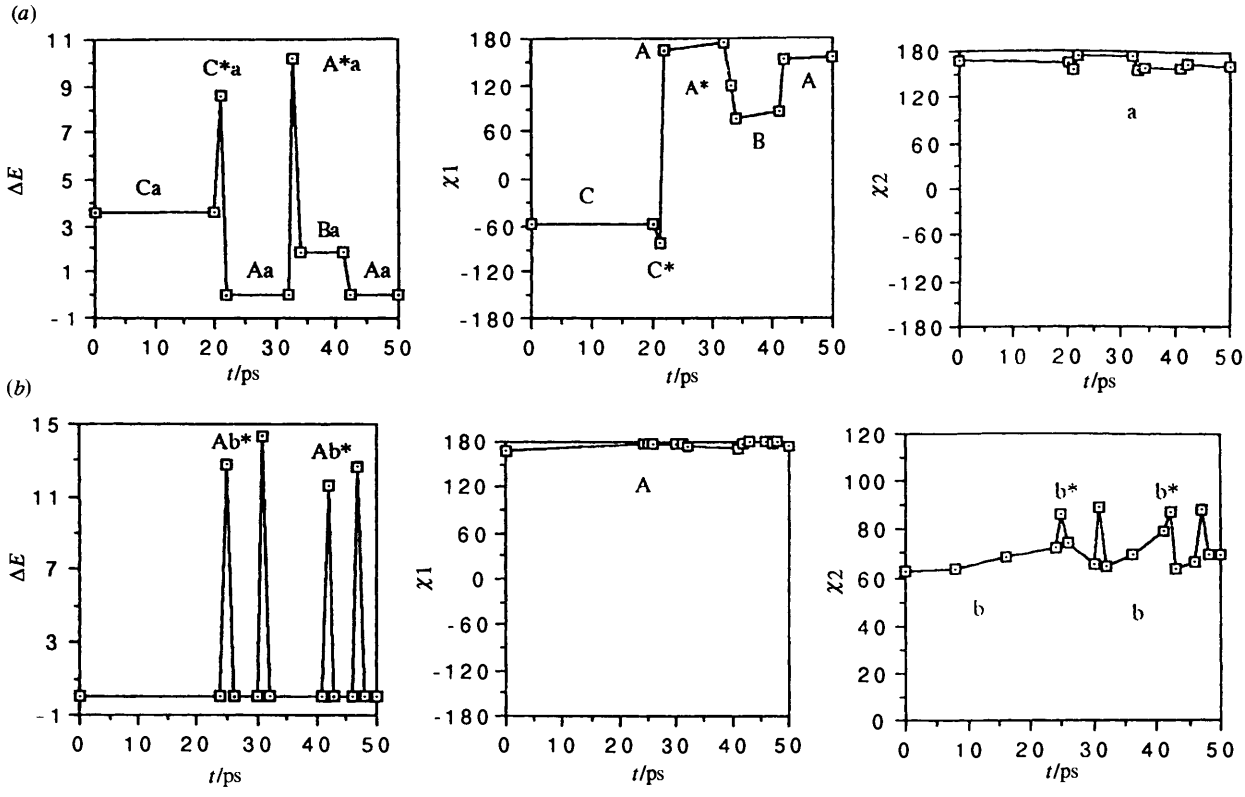

Fig. 5 The 50 ps MD run at 300–600 K in a water box relative to **4T**, favoured during the trajectory some 'less-staggered' rotamers which represent high-energy intermediates neighbouring to the transition state. They are almost in an 'eclipsed' form, represented by the symbol (*). (*a*) They represent a particular transition state implied in the interconversion of rotamers: C→C*→A→A*→B. The difference between **C*a** and **Ca** or between **A*a** and **Aa** corresponds to a (−85°) *gauche* torsion angle instead of (−57°) according to the staggered rotors '**C**' or with a (134°) *trans* torsion angle instead of (175°) according to the staggered rotors '**A**'. (*b*) The MD run relative to **4T** show that four intermediate **Ab*** structures are generated (a 90° *gauche* torsion angle instead of 65° according to the staggered rotors '**b**'). The variation of their high-energy is a function of both rotations about the two planes of carboxylate groups, α- and γ-CO_2^- groups. The planes take different orientations searching to favour the interconversion of rotamers. The amplitude of movement of carboxylate groups leads to another low-energy structure **Ab**, presenting a 'turned-back' α-CO_2^- and γ-CO_2^-, but does not allow the interconversion to take place. High rotational barriers have to be passed for the **4T** isomer to observe the rotational conversion since an important electrostatic (the α-NH_3^+ and the γ-CO_2^- groups) and steric contributions in **4T** leads to a very good stabilization of the **Ab** conformation.

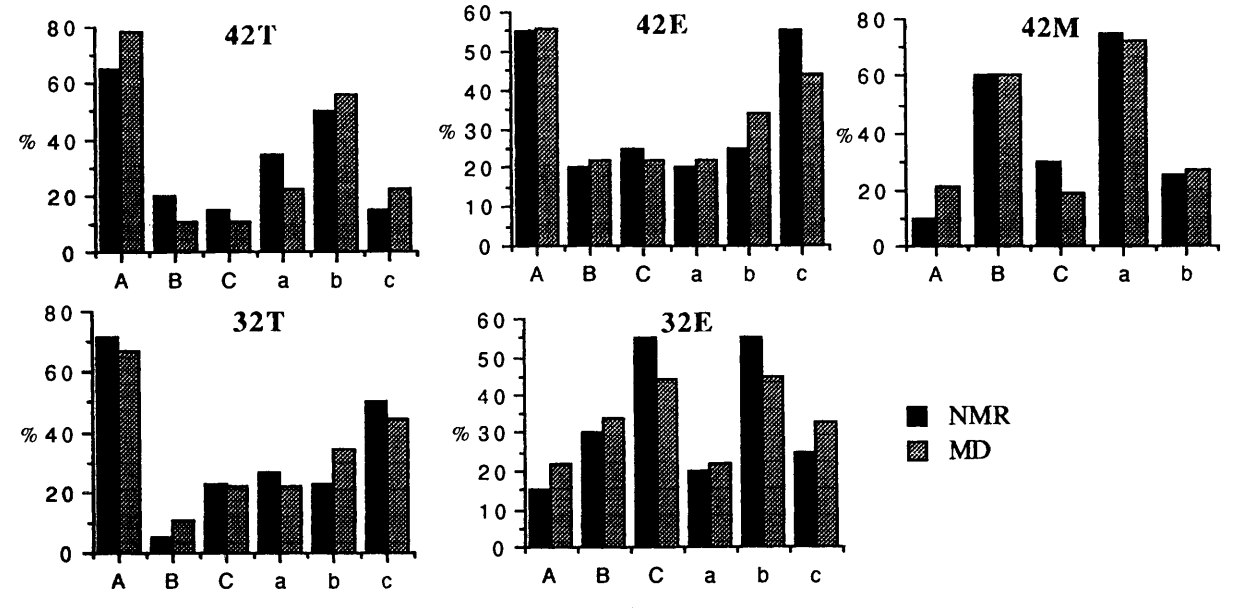

Fig. 6 Correlation between the observed (NMR) and calculated (MD) probabilities of the rotamers of the five isomers (**3T**, **3E**, **4T**, **4E** and **4M**), using the population of rotamers calculated from the MD runs of Table 6

The preferred conformations of the studied compounds (**3T**–**4M**) are characterized by physical features of the potentially active functional groups (Figs. 7 and 8), such as the interatomic distances d_1 (α-NH_3^+–γ-CO_2^-) and d_2 (α-CO_2^-–γ-CO_2^-), the repartition of alkyl chain torsion angles χ1 [α-CO_2^-–C(2)–C(3)–C(4)], χ2 [C(2)–C(3)–C(4)–γ-C_2^-] and the coordinates *x*, *y* and *x*, *z* of characteristic functional atoms α-N, α-C, γ-C (Table S4 of supplementary material).

The molecular modelling calculations on the **4T** zwitterion indicate that the most stable conformation is one in which the

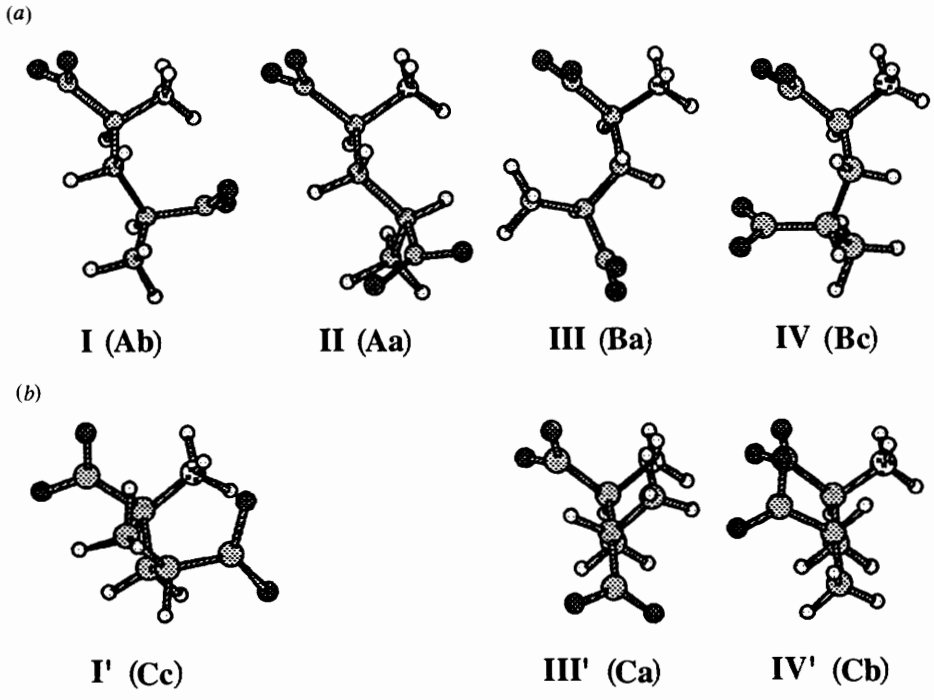

Fig. 7 Representation of the different conformational families **I**, **II**, **III** and **IV** corresponding respectively to **Ab** (or Aβ), **Aa**, **Ba** (or **Bb**, Bβ) and **Bc** (or **B**α) and the family **I'**, **III'** and **IV'** corresponding respectively to **Cc** (or **C**α, **Ac**, **A**α), **Ca** and **Cb** (or **C**β)

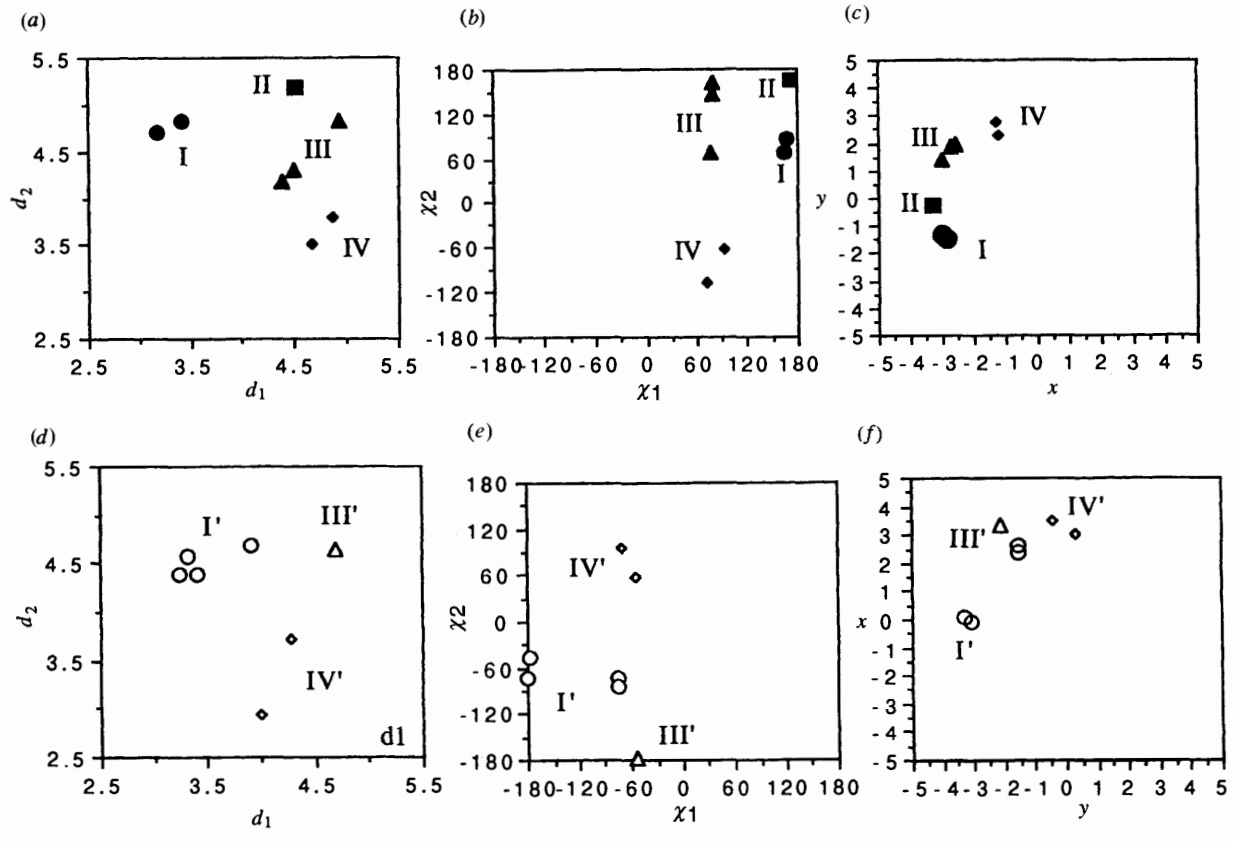

Fig. 8 **I** (●), **II** (■), **III** (▲), **IV** (◆) and **I'** (○), **III'** (△), **IV'** (◇). The different conformational families identified from the NMR and MD data of the five analogues are represented in a diagram according to the physical features (Tables S4 and S5 of supplementary material) of the potentially active functional groups; (*a*) the three-dimensional interatomic distances between involved atoms, $d_{1(\alpha\text{-}NH_3^+\text{-}\gamma\text{-}CO_2^-)}$, $d_{2(\alpha\text{-}CO_2^-\text{-}\gamma\text{-}CO_2^-)}$; (*b*) the repartition of alkyl chain torsion angles $\chi 1$, $\chi 2$; (*c*) the coordinates *x*, *y*; (*d*) the three-dimensional interatomic distances between involved atoms, $d_{1(\alpha\text{-}NH_3^+\text{-}\gamma\text{-}CO_2^-)}$, $d_{2(\alpha\text{-}CO_2^-\text{-}\gamma\text{-}CO_2^-)}$, (*e*) the repartition of alkyl chain torsion angles $\chi 1$, $\chi 2$ and (*f*) the coordinates *x*, *z* of characteristic functional atoms α-N, α-C, γ-C.

molecule has torsion angles $\chi 1$ [α-CO_2^-–C(2)–C(3)–C(4)] of 180° and $\chi 2$ [C(2)–C(3)–C(4)–γ-CO_2^-] of 60°. This is the most populated conformation in NMR solution. The conformation *tg* ($\chi 1$ = 180° and $\chi 2$ = 60°) is 80% populated, whereas the folded conformations *gg* and the very extended *tt* are 10% populated. This agreement probably arises because the calculations have included the hydration effects of the aqueous solvent. A similar result is obtained for **3T** and **4E**, (*tg* with

$\chi 2 = -60°$) but a reverse percentage between *gg* and *tg* conformations is observed for **3E** and **4M**.

Rather than classify the conformational populations by combinations of symbols *t* and *g* they are grouped in a second step according to the distance (d_1) between the positively charged N atom and the carbon atom of the γ-CO_2^- group, but pairs with the same $^+N\cdots\gamma$-CO_2^- distance will differ in the distance between carboxylate groups (d_2).[31] The fully extended form (d_1 around 5 Å) is unique (**Ba** or **B**α) and very slightly populated except for **4E** (20%) and **4M** (60%). There are four conformations (**Ab**, **Ac**, **Cb**, **Cc**) with the shorter $^+N\cdots CO_2^-$ distances of 2.5 to 3.9 Å which comprise nearly 80% of the solution conformations of **4T** (**Ab** essentially, **Ac** and **Cc**), **4E** and **3T**. Relative to d_2, the most populated conformations (80%) in **4T** solution are ones with the distance d_2 (α-$CO_2^-\cdots\gamma$-CO_2^-) around 4.2 Å (**Ab**, **Ac** and **Ba**). The fully extended form relative to the carboxylic groups (d_2 around 5 Å) is unique (**Aa**) and very slightly populated (10% for **4T** and **3T**) and the folded form with the shorter α-$CO_2^-\cdots\gamma$-CO_2^- distance (d_2 around 3 Å) is only found in the **Bc** or **Cb** conformations for **3E**.

Thus, the conformational populations have been classified according to the distances between functional groups. Two groups are considered in electrostatic interaction if their distance is less than (or equal to) 4 Å. In order to keep a limited number of classes (**I**–**IV**) (Fig. 8) two families will be characterized by a d_1 distance shorter than d_2: **I** ($d_1 \ll d_2$) and **II** ($d_1 < d_2$). Conversely, two other families will be characterized by a d_2 distance shorter than d_1: **III** ($d_2 < d_1$) and **IV** ($d_2 \ll d_1$). These four families (Type **I**–**IV**) essentially characterized by the two interatomic distances (Å) d_1 and d_2 present torsion angles $\chi 1$ [α-CO_2^-–C(2)–C(3)–C(4)] from +60 to 180° and $\chi 2$ [C(2)–C(3)–C(4)–γ-CO_2^-] from −120 to 180°. But other families (Type **I'**–**IV'**) with the same d_1, d_2 distances will differ by the alkyl chain torsion angles $\chi 1$ (from −180 to −60°), $\chi 2$ (from −180 to 120°) and by the coordinates *x*, *y* and *x*, *z* of characteristic functional atoms α-N, α-C, γ-C (Figs. 7 and 8). For a nearly equivalent position of the two functional groups, the α-N and α-C(α-CO_2^-) as it is shown in Fig. 8, one can observe that the conformational swinging of the γ-carboxylate group for families **I**–**IV** corresponds to an exploration from the right to the left clockwise with respect to the representation on Fig. 8. While for families **I'**–**IV'** this exploration corresponds to a perpendicular plane. The families (Type **I'**–**IV'**) with these characteristics are populated to about 20% in **4T** solution, whatever the pH is. They represent 50–80% of the other **3T**, **3E** and **4E** isomers, solution protonated or unprotonated.

Conclusions

The experiments have essentially provided useful basic information. MD has the advantage of taking into account NMR results by revealing correlations in conformation about the two bonds which cannot be revealed by the NMR analysis. This aspect has to be considered, given the importance of a comparative study (NMR–MD) even for small charged molecules, in deciding which conformation is more populated than the other at a certain temperature in a specific solvent. The solvent effect leads to the coexistence of stacked and extended forms in water in very satisfactory agreement with NMR solution findings.

The analogues of glutamic acid are flexible and they exhibit specific conformational averaging in solution. The results of the present study underline the specificity of the influence of electrostatic and steric interactions for each compound. The conformation depends strongly on substitution, the solvent and the pH.

(i) A detailed analysis of the conformations showed that the coexistence of ammonium (α-NH_3^+) and carboxylate (γ-CO_2^-), or carboxylate (α-CO_2^-) and carboxy groups (γ-CO_2H), within one structure led to the appearance of stacked conformations, such as **Ab** (Type **I**) and **Bb** (Type **III**), respectively. The electrostatic interaction between the α-NH_3^+ and the γ-CO_2^- groups at neutral pH stabilized the **Ab** conformation (Family **I**), and when the γ-CO_2^- group is protonated, one new interaction with the α-CO_2^- is established, thus favouring another conformation **Bb** (Family **III**).

(ii) Hydrogen atoms and methyl and α-amino groups take up an orientation such that there is no interaction between the two bulky groups and steric hindrance is weak. The population of the '*anti*' rotamer '**A**' relative to the $\chi 1$ torsion angle is predominant in aqueous solution when the α-carboxy group has an extended orientation which favours a zig-zag alkyl chain[32] α-C(1)–C(2)–C(3)–C(4)–C(4-Me). The conformations differ in the other compounds by the methyl (or methylene) position, that increases steric bulk and lipophilicity near the potential active groups and not at the end of the alkyl chain. A different configuration of the methyl group corresponds in MD calculations to a loss of 2–3 kcal mol^{-1}. These modifications seem to be crucial for the ligand–receptor recognition mechanism.

Experimental

Nuclear magnetic resonance

All NMR spectra were recorded on a Bruker AMX-500 spectrometer equipped with an X32 computer. A sample of **3T**, **3E**, **4T**, **4E** or **4M**[19] (7.4 mg) was dissolved in 0.6 ml of D_2O to give a final concentration 0.09 mol dm^{-3} for the different isomers. The pH (pD = pH − 0.4, uncorrected here) was adjusted by addition of DCl or NaOD. At pH 7 the samples were dissolved in an aq. NaD_2PO_4–Na_2DPO_4 buffer, and it was possible to attain concentrations of 0.09 mol dm^{-3} for the ^1H and ^{13}C experiments.

The errors on the chemical shifts are 0.01 and 0.1 ppm for ^1H and ^{13}C respectively. A crystal of 3-(trimethylsilyl)[2,2,3,3-$^2H_4$]propionic acid, sodium salt ([$^2H_4$]TSP) was used as internal reference for the proton shifts, and for the carbon a value of the absolute frequency was used. The coupling constants are given with a precision of 0.5 Hz. The spectrum simulation was performed on a Macintosh II computer using the software NMR II. Presaturation of the solvent was used for all the 1D and 2D ^1H experiments. Four spectra from 280 to 310 K were recorded.

The Selective Inept (INAPT)[20b] recorded with 32K data points with a selective excitation of the Me and 2-H protons allowed us to differentiate carbons. The ^1H detected ^1H, ^{13}C HMBC spectrum[33] (GE-HMQC, gradient-enhanced heteronuclear multiple-quantum correlation) was recorded at 300 K with 16 scans, 256 experiments of 1024 data points, a sweep width of 4000 Hz in f_2 and 27507 Hz in f_1. One millisecond half-sinusoid gradients of 28, 28, and −14 G cm^{-1} were used to select for protons attached to carbon and a delay of 80 ms which was optimum for two- or three-bond couplings.

The 2D *J*δ selective INEPT[22] using the polarisation transfer from ^1H to ^{13}C gave long-range heteronuclear coupling constants $^3J(^{13}C–^1H)$. The selective excitation of a proton signal allows detection of a single doublet for the corresponding coupled carbon(s). At 500 MHz, selectivity was achieved by a DANTE-type pulse train generated by the decoupler channel. In this study, the $^3J(^{13}C–^1H)$ coupling constants were measured for the two rotors: the 2-H proton was excited for the H(2)–C(2)–C(3)–C(4) and the 4-H proton for the H(4)–C(4)–C(3)–C(2), but if ambiguity remained as to the assignments of the individual diastereotopic protons, we used their corresponding $^3J(^{13}C–^1H)$ coupling constants to determine their assignments. This experiment also allows us to analyse the '**A**, **B**, **C**' and the '**a**, **b**, **c**' rotamer populations. This experiment was recorded at 300 K with 256 scans of 4000 data points, 64 experiments, a spectral width of 220 ppm in f_2 and 62.5 Hz in f_1.

Computer simulations

The conformations of the methylated α-amino acid compounds that were incorporated into the analysis were obtained using the BIOSYM molecular modelling software on a Silicon Graphics workstation.

Initial structures were built using the INSIGHT II builder module, which directly produced coarse three-dimensional starting structures. To mimic ionization at neutral pH, an sp^3 hybridization was assigned to the amine of the main alkyl chain, increasing the molecular electrostatic total charge by +1.

To mimic the solvent effect, the relative permittivity was set to be distance-dependent, $\varepsilon = R_{ij}$ ($\varepsilon = 5$)[28] in the description of the coulombic interaction. A second protocol can be used with explicit solvent molecules incorporated during the run. We constructed solvation boxes containing the glutamate analogue molecule and several water molecules using periodic boundary conditions. A cut-off function of 11 Å was applied for non-bonded interactions. The relative permittivity was set to $\varepsilon = 1$ and a box contained 48 (12-12-12) water molecules. The energies obtained are those of 'molecule +48 H_2O' systems.

Energy minimization and MD simulations were performed with the INSIGHT II Discover module,[34] using the consistent valence force field (CVFF).

The first step in the modelling consisted of minimizing the structure previously constructed, to find a local energy minimum on the potential energy hypersurface of the molecule. Calculations were performed according to several algorithms commonly used in molecular mechanics for choosing descent directions, namely steepest descent and conjugate gradient methods.

The second step of the conformational sampling procedure consisted of recording MD trajectories. By solving the equations of motion for a system of atoms, MD has an advantage in that it is not restricted to harmonic motion about a single minima but allows molecules to cross energy barriers and explore other stable conformations. Molecular conformers were sampled during a 100 ps MD trajectory at 300 K with 48 water molecules. A time step of 1 fs was used, and the system was equilibrated for 4 ps. A conformation was stored each 1 ps so that 100 conformations with 48 water molecules were recorded by the end of the MD simulation. A previous run was performed with a 4 ps equilibration period, in which the system was coupled to a thermal bath at 300 K to relieve strains in the structure and reach thermodynamic equilibrium. The simulation was then continued by a 8 ps period at 300 K followed by a temperature jump at 600 K during 4 ps. The 50 ps trajectory is sampled every picosecond and the remaining structures are then minimized by molecular mechanics and stored. The final conformers found with lowest energies were then further minimized to a gradient less than 0.01 kcal mol^{-1} $Å^2$ to obtain their energies at higher accuracy. A second set of simulations have been made without any temperature jumps at 300 K during 100 ps, with energy minimisation each ps as above.

The sampling every picosecond was supposed sufficiently large for a significant moving of the atoms and sufficiently short for a correct sampling of the conformational space. For an isolated molecule, the experiment takes about 15–30 min. For experiments in which the molecules are introduced into the solvation boxes, the CPU times are much longer, *i.e.* 24 or 48 h, according to the protocol.

All molecular conformations were compared using the Analysis module of INSIGHT II. Conformational similarities were evaluated by calculating the RMS deviation between heavy atoms for each possible pair of the different structures. The results represent groups of stuctures whose small RMS deviations (< 1 Å) suggested that they may belong to the same conformational family. Conformational representatives extracted from each family were compared for each compound, using a superimposition procedure.

Coupling constants were calculated from the torsion angles using the software ALTONA on a Macintosh II computer.[35]

Acknowledgements

We are grateful to B. Champion and Dr P. Ladam for helpful advice and we thank J. Hart-Davis for skilful assistance.

References

1 (*a*) D. W. Choi and S. M. Rothman, *Annu. Rev. Neurosci.*, 1990, **13**, 171; (*b*) J. C. Watkins, P. Krogsgaard-Larsen and T. Honoré, *Trends Pharmacol. Sci.*, 1990, **11**, 25.
2 (*a*) S. Nakanishi, *Science*, 1992, **258**, 597; (*b*) T. V. P. Bliss and G. L. Collingridge, *Nature*, 1993, **361**, 31.
3 B. Meldrum and J. Garthwaite, *Trends Pharmacol. Sci.*, 1990, **11**, 379–387.
4 (*a*) D. T. Monoghan, R. J. Bridges and C. W. Cotman, *Annu. Rev. Pharmacol. Toxicol.*, 1989, **29**, 365; (*b*) R. H. Evans and J. C. Watkins, *Annu. Rev. Pharmacol. Toxicol.*, 1981, **21**, 165; (*c*) B. Sommer and P. H. Seeburg, *Trends Pharmacol. Sci.*, 1992, **13**, 291.
5 E. Palmer, D. T. Monoghan and C. W. Cotman, *Eur. J. Pharmacol.*, 1989, **166**, 585.
6 (*a*) D. D. Schoepp and P. J. Conn, *Trends Pharmacol. Sci.*, 1993, **14**, 13; (*b*) J. P. Pin and R. Duvoisin, *Neuropharmacology*, 1995, **34**, 1; (*c*) J. P. Pin and J. Bockaert, *Curr. Opin. Neurobiol.*, 1995, in the press; (*d*) T. Knöpfel, R. Kuhn and H. Allgeier, *J. Med. Chem.*, 1995, **38**, 1417.
7 (*a*) T. Abe, H. Sugihara, H. Nawa, R. Shigemoto, N. Mizuno and S. Nakanishi, *J. Biol. Chem.*, 1992, **267**, 13361; (*b*) Y. Tanabe, M. Masu, T. Ishii, R. Shigamoto and S. Nakanishi, *Neuron*, 1992, **8**, 169.
8 (*a*) I. Aramori and S. Nakanishi, *Neuron*, 1992, **8**, 757; (*b*) Y. Hayashi, Y. Tanabe, I. Aramori, M. Masu, K. Shimamoto, Y. Ohfune and S. Nakanishi, *Br. J. Pharmacol.*, 1992, **107**, 539; (*c*) Y. Tanabe, A. Nomura, M. Masu, R. Shigemoto, N. Mizuno and S. Nakanishi, *J. Neurosci.*, 1993, **13**, 1372.
9 (*a*) Y. Nakajima, H. Iwakabe, C. Akazawa, H. Nawa, R. Shigemoto, N. Mizuno and S. Nakanishi, *J. Biol. Chem.*, 1993, **268**, 11 868; (*b*) N. Okamoto, S. Hori, C. Akazawa, Y. Hayashi, R. Shigemoto, N. Mizuno and S. Nakanishi, *J. Biol. Chem.*, 1994, **269**, 1231.
10 (*a*) M. Masu, Y. Tanabe, K. Tsuchida, R. Shigemoto and S. Nakanishi, *Nature*, 1991, **349**, 760; (*b*) K. M. Houamed, J. L. Kuijper, T. L. Gilbert, B. A. Haldeman, P. J. O'Hara, E. R. Mulvihill, W. Almers and F. S. Hagen, *Science*, 1991, **252**, 1318; (*c*) D. F. Ortwine, T. C. Malone, C. F. Bigge, J. T. Drummond, C. Humblet, G. Johnson and G. W. Pinter, *J. Med. Chem*, 1992, **35**, 1345; (*d*) P. J. O'Hara, P. O. Sheppard, M. Thogersen, D. Venezia, B. A. Haldeman, V. Mc Crane, K. M. Houamed, C. Thomsen, T. L. Gilbert and E. R. Mulvihill, *Neuron*, 1993, **11**, 41; (*e*) G. Costantino, B. Natalini, R. Pellicciari, F. Moroni and G. Lombardi, *Bioorg. Med. Chem.*, 1993, **4**, 259.
11 (*a*) F. Sladeczek, J. P. Pin, M. Recasens, J. Bockaert and S. Weiss, *Nature*, 1985, **317**, 717; (*b*) F. Sladeczek, M. Recasens and J. Bockaert, *Trends Neurosci.*, 1988, **11**, 545; (*c*) D. D. Schoepp, J. Bockaert and F. Sladeczek, *Trends Pharmacol. Sci.*, 1990, **11**, 508.
12 (*a*) K. R. Stratton, P. F. Worley and J. M. Baraban, *Eur. J. Pharmacol.*, 1989, **173**, 235; (*b*) C. Thomsen, P. Kristensen, E. Mulvihill, B. Haldman and P. D. Suzdak, *Eur. J. Pharmacol.*, 1992, **227**, 361.
13 (*a*) J. P. Pin, C. Waeber, L. Prézeau, J. Bockaert and S. F. Heimann, *Proc. Natl. Acad. Sci. USA*, 1992, **89**, 10 331; (*b*) J. P. Pin, J. Bockaert, K. M. Pittaway and D. C. Sunter, unpublished results.
14 Z. Q. Gu, D. P. Hesson, J. C. Pelletier, M. L. Maccechini, L. M. Zhou and P. Skolnick, *J. Med. Chem*, 1995, **38**, 2518.
15 (*a*) A. Meister, *Harvey Lect.*, 1969, 139; (*b*) H. M. Kagan and A. Meister, *Biochemistry*, 1966, **5**, 725; (*c*) H. M. Kagan and A. Meister, *Biochemistry*, 1966, **5**, 2423.
16 F. Pratviel-Sosa, F. Acher, F. Trigalo, D. Blanot, R. Azerad and J. van Heijenoort, *FEMS Microbiol. Lett.*, 1994, **115**, 223.
17 F. Pratviel-Sosa, D. Mangin-Lecreulx and J. van Heijenoort, *Eur. J. Biochem.*, 1991, **202**, 1169.
18 N. S. Ham, *Molecular and Quantum Pharmacology*, eds. E. Bergmann and B. Pullman, Dordrecht, Holland, 1974, pp. 261–268.
19 (*a*) F. Acher and R. Azerad, *Tetrahedron: Asymmetry*, 1994, **5**, 731; (*b*) F. Trigalo, C. Molliex, B. Champion and R. Azerad, *Tetrahedron Lett.*, 1991, **32**, 3049.
20 (*a*) M. R. Bendall and D. T. Pegg, *J. Magn. Reson.*, 1983, **53**, 272; (*b*) A. Bax, *J. Magn. Reson.*, 1984, **57**, 314; (*c*) L. J. Linand and G. A. Cordell, *J. Chem. Soc., Chem. Commun.*, 1986, 377.

21 (*a*) A. De Marco, M. Llinas and K. Wüthrich, *Biopolymers*, 1978, **17**, 637; (*b*) G. C. K. Roberts and O. Jardetzky, *Adv. Protein Chem.*, 1970, **24**, 447; (*c*) O. Jardetzky and G. C. K. Roberts, *NMR in Molecular Biology*, Academic Press, New York, 1981, pp. 147–150; (*d*) P. E. Hansen, J. Feeney and G. C. K. Roberts, *J. Magn. Reson.*, 1975, **17**, 249.
22 P. Ladam, J. Gharbi-Benarous, M. Pioto, M. Delaforge and J. P. Girault, *Magn. Reson. Chem.*, 1994, **32**, 1.
23 C. Altona and M. Sundaralingam, *J. Am. Chem. Soc.*, 1973, **95**, 2333; F. A. Haasnoot, A. M. de Leeuw and C. Altona, *Tetrahedron*, 1980, **36**, 2783.
24 (*a*) A. De Marco, M. Llinas and K. Wüthrich, *Biopolymers*, 1978, **17**, 2727; (*b*) A. De Marco and M. Llinas, *Biochemistry*, 1979, **18**, 3846.
25 I. Tvaroska, M. Hricovini, E. Petrakova, *Carbohydr. Res.*, 1989, **189**, 359.
26 K. G. R. Pachler, *Spectrochim. Acta*, 1964, **20**, 581.
27 S. K. Burt, D. Mackay and A. T. Nagler, in *Computer-Aided Drug Design*, eds. T. J. Perun and C. L. Propst, Marcel Dekker, New York and Basel, 1989, p. 66.
28 N. Morelle, J. Gharbi-Benarous, F. Acher, G. Valle, M. Crisma, C. Toniolo, R. Azerad and J. P. Girault, *J. Chem. Soc., Perkin Trans. 2*, 1993, 525; F. Acher, N. Morelle, J. Gharbi-Benarous, G. Valle, M. Crisma, C. Toniolo, R. Azerad and J. P. Girault, *Peptides*, 1993, 581.
29 (*a*) M. Karplus and G. A. Petsko, *Nature*, 1990, **347**, 631; (*b*) W. F. van Gunsteren and H. J. C. Berendsen, *Angew. Chem., Int. Ed. Engl.*, 1990, **29**, 992; (*c*) M. P. Allen and D. J. Tildesley, *Computer Simulation of Liquids*, Oxford Science Publications, 1991; (*d*) C. L. Brooks, M. Karplus and B. M. Pettitt, *Proteins. A Theoretical Perspective of Dynamics, Structure and Thermodynamics*, Wiley, New York, 1988.
30 P. Kollmann, *J. Am. Chem. Soc.*, 1984, **106**, 765.
31 V. Larue, J. Gharbi-Benarous, F. Acher, G. Valle, M. Crisma, C. Toniolo, R. Azerad and J. P. Girault, *J. Chem. Soc., Perkin Trans. 2*, 1995, 1111.
32 G. M. Underwood and C. A. Kingsbury, *J. Chem. Soc., Perkin Trans. 2*, 1973, 947.
33 R. E. Hurd and B. K. John, *J. Magn. Reson.*, 1991, **91**, 648.
34 P. Dauber-Osguthorpe, V. A. Roberts, D. J. Osguthorpe, J. Wolff, M. Genest and A. T. Hagler, *Proteins: Struct. Funct. Genet.*, 1988, **4**, 31.
35 C. M. Cerda-Garcia-Rojas, L. G. Zepeda and P. Joseph-Nathan, *Tetrahedron Comput. Methodol.*, 1990, **3**, 113.

Paper 6/00458J
Received 22*nd January* 1996
Accepted 20*th March* 1996